IEEE Access
Multidisciplinary | Rapid Review | Open Access Journal

Received July 26, 2021, accepted August 8, 2021, date of publication August 16, 2021, date of current version August 30, 2021.

Digital Object Identifier 10.1109/ACCESS.2021.3104904

Representation of Voltage-Controlled Devices in Reduced Modeling of Distribution Networks

GIOVANNI MERCURIO CASOLINO, (Member, IEEE), AND ARTURO LOSI
Dipartimento di Ingegneria Elettrica e dell'Informazione "Maurizio Scarano," University of Cassino and Southern Lazio, 03043 Cassino, Italy
Corresponding author: Giovanni Mercurio Casolino (casolino@unicas.it)

This work was supported by the Italian Ministero dell'Istruzione, dell'Università e della Ricerca (MIUR) program "Dipartimenti di Eccellenza 2018–2022."

ABSTRACT The number of distributed energy resources is continuously increasing, which makes the study of distribution systems increasingly demanding; a reduced yet accurate network modeling could be beneficial in terms of computational effort, and of information treatment burden as well. With a traditional approach, the presence of numerous voltage-controlled devices limits the possibility of obtaining a significantly reduced representation of the network, due to the need to keep the voltage of the nodes to which they are connected. In this paper, we propose two approaches for obtaining and solving the reduced model of a distribution network with numerous devices with voltage-controlled power injection. The application of the two approaches to four test cases highlights the acceptability of the approximations introduced by the reduction of the model and the computational aspects of the solution of the reduced model. The results put into evidence the practicability of the proposed approaches, as well as the associated computational benefits.

INDEX TERMS Distribution network reduced modeling, unbalanced systems, voltage-controlled devices.

NOMENCLATURE

The principal symbols and names used in the paper are:

$*$	Reference value.
$\widehat{\ }$	Complex conjugate.
$\odot$	Element-wise matrix product.
$diag\{x_i\}$	Diagonal matrix whose principal diagonal is made of the components of vector x.
$\dot{\alpha}_{i\_\phi,h}$	Factor for active power.
$\dot{\beta}_{i\_\phi,h}$	Factor for reactive power.
$\bar{\delta}$	Voltage corrections.
λ_h	Mean slope of the h-th volt-var control law.
$\nu_{h,k}$	Number of phases to which the k-th prosumer of the h-th category is connected.
$\pi^*_{h,k}, q^*_{h,k}$	Fixed share of the active and reactive power injection by the k-th prosumer in the h-th category.
$\varphi^*_{h,k}$	Phase angle (assumed constant) of the load current of the k-th prosumer in the h-th category.
$\dot{A}_h$	n_{LA} vector of factors $\dot{\alpha}_{i\_\phi,h}$.
$\dot{B}_h$	n_{LA} vector of factors $\dot{\beta}_{i\_\phi,h}$.
$\dot{\Pi}, \dot{\Psi}, \dot{\Upsilon}, \dot{X}$	Compacted network matrices.
bus	A group of nodes in the same location; it may consist of one to three nodes.
d	Describing nodes.
e	Edge nodes.
$f_h(P_h)$	Relationship between active and reactive powers for the h-th category.
$g_{h,k}(U)$	Volt-var control law for the k-th prosumer of the h-th category.
$\widetilde{g}_h(U)$	Volt-var control law for the h-th category.
in	Nodes/busses other than the describing ones.
n_a, n_b	Number of categories of prosumers of type N_A or N_B, respectively.
n_h	Number of prosumers in the h-th category.
n_D	Number of D nodes.
n_{LA}	Sum of the number of phases in all Load Area busses.
node	A single phase in a bus.
q	Nodes not in d with reactive generation depending on voltage.
$p^*_{h,k}, q^*_{h,k}$	Fixed share of the active and reactive power injection by the k-th prosumer in the h-th category.

The associate editor coordinating the review of this manuscript and approving it for publication was Payman Dehghanian.

r	Suffix: Rated value.
s_g	Dimensionless mean slope of volt-var control laws.
D	d and q nodes.
$\widetilde{G}_h(U)$	n_D vector whose i-th term is the function $\widetilde{g}_h(\cdot)$ evaluated with the i-th voltage.
I	Identity matrix.
$\bar{J}$	Injected currents.
$\bar{J}^{ext}$	Currents from the outside of the Load Area.
$\bar{J}^{p}$	Prosumers' injected currents.
$\bar{J}^{p}_{i\_\phi}$	Prosumers' injected current at the ϕ–th phase of the i–th bus.
M^k, N^k	Square matrices at the k-th iteration.
N_A, N_B	Categories of prosumers whose reactive power depends on active power or on voltage, respectively.
P_h, Q_h	Active and reactive powers injection of the h-th category.
$P_{h,k}$, $Q_{h,k}$	Active and reactive power injections by the k-th prosumer in the h-th category.
$P^{inj}_{i\_\phi}$, $Q^{inj}_{i\_\phi}$	Active and reactive power injections in the ϕ-th phase of the i–th bus.
P_L	Active power consumption of the pure load prosumer's category.
R	Suffix: Reduced.
$\bar{U}$	Nodal voltages.
$\bar{U}_{i\_\phi}$	Voltage of the ϕ–th phase of the i–th bus.
$U_{node,\,hk}$	Voltage amplitude of the node where the k-th prosumer of the h-th category is connected to the grid.
$\dot{Y}$	Admittance matrix.

I. INTRODUCTION

The study of distribution systems is becoming more and more demanding, as models grow in complexity and dimension, mainly due to the increasing number of distributed generators and the exploitation of prosumers' flexibility. In the planning of distribution systems, new approaches are adopted which require a huge amount of operations simulations [1]. Real-time simulations are carried out to study the operational behavior of physical devices without interfering with the actual distribution grid [2]. New monitoring and control functionalities make available a large amount of information, which must be adequately treated [3], [4]. In all cases, benefits can accrue from a reduced (yet accurate) grid modeling, as it allows to reduce the computational time and the burden of information treatment.

The approach of Load Area (LA) [5], [6] can be adopted: LAs are subgrids identified as clusters of nodes whose power injection has a similar impact on the network operating conditions; a LA can comprise a whole distribution grid [7]. In each LA the relevant busses can be selected and a reduced network model can be obtained for the LA [8].

Starting from [9], network reduction is regularly revisited; recently, attention is paid to the simplification of the modeling of distribution networks [1], [2], [10]–[14]. The nodes where the reactive (and possibly even the active) injection is voltage-controlled should be retained, for a correct representation of the control laws. This makes it difficult to get a reduced model with good computational speed-ups when the number of such voltage-controlled devices is significant [15]. Recently, some methods have been presented that address this issue; in this paper, new approaches to the problem are proposed.

Compared to [16], in this study no optimization problem is solved at each time step to obtain the aggregate control curve for all voltage-controlled devices represented in an aggregated node, and individual voltage-controlled devices are explicitly represented. In [15] the voltage of the to-be-reduced nodes with voltage-controlled power injection devices are obtained by means of an estimation through sensitivities, while in the present study the voltages are explicitly obtained.

In this paper, two methods to represent the voltage-controlled power injection in a reduced modeling of distribution systems are proposed, which are useful to take into account any type of voltage-based control law for power injection of devices installed in the to-be-reduced nodes. In one method, the modeling of voltage-controlled devices is the usual one, and computational benefit can derive from the newly proposed algorithm. In the second method, a new modeling of volt-var control laws installed in the to-be-reduced nodes is proposed together with a specific algorithm.

This work contributes to the problem of representing the units with voltage-controlled power injection in network reduction mainly with:

- straightforward treatment of voltage-var control laws;
- no need of introducing equivalent reactive generation;
- little need for matrix inversions;
- relevant reduction of computational effort.

The details of the methods are presented, and the reduced relationships among relevant voltages/currents are obtained. The methods are applied to four test cases of different sizes, highlighting the computational aspects related to the reduced network modeling and solution.

II. MODELING OF PROSUMERS

The modeling of the power injections by prosumers in three-phase unbalanced systems is presented; it is based on the modeling proposed in [13], [14], with the addition of prosumers with voltage-controlled reactive power injection.

A. PROSUMERS

In a given LA, similar prosumers (residential, commercial, etc.) are grouped into categories [8], [17].

Active power

The active power injection by the k-th prosumer in the h-th category can be assumed to be a fixed share of the active power injection of the whole category:

$$P_{h,k} = p^*_{h,k} P_h, \quad h \in N_A,\ h \in N_B,\ k \in n_h. \tag{1}$$

The reactive power injection by the same prosumer can be expressed as a function of either its active power injection or of the voltage at its terminals, depending on the characteristics of the prosumer.

Reactive power as a function of active power

The reactive power injection depending on the active power injection can be put as:

$$Q_{h,k} = q^*_{h,k} f_h(P_h) P_h, \quad h \in N_A,\ k \in n_h; \tag{2}$$

the details of such relationships for different prosumers' categories can be found in Appendix A.

For the subsequent development it is useful to put (2) as

$$Q_{h,k} = q^*_{h,k} \widetilde{f}_h(P_h), \quad \widetilde{f}_h(P_h) = f_h(P_h) P_h,\ h \in N_A,\ k \in n_h. \tag{3}$$

Reactive power as a function of nodal voltage

As the penetration of DG increases, grid codes may require that they assist in voltage regulation. A volt-var control scheme is realized through a fixed control curve programmed in the DG inverter [18], [19], so that:

$$Q_{h,k} = g_{h,k}(U_{node,hk}) Q^r_{h,k}, \quad h \in N_B,\ k \in n_h. \tag{4}$$

For any given category in the N_B set, it can be assumed that all prosumers behave according to the same control law

$$g_{h,k}(U_{node,hk}) = g_h(U_{node,hk}), \quad h \in N_B,\ k \in n_h; \tag{5}$$

the details of functions $g_h(U_{node,hk})$ can be found in Appendix B. Moreover, the rated value of reactive power of any prosumer in a given category is a known share of the total rated reactive power of its category:

$$Q^r_{h,k} = q^*_{h,k} Q^r_h, \quad \in N_B,\ k \in n_h. \tag{6}$$

From (4)–(6) it follows that:

$$\begin{aligned} Q_{h,k} &= g_h(U_{node,hk}) q^*_{h,k} Q^r_h \\ &= q^*_{h,k}\, \widetilde{g}_h(U_{node,hk}), \quad h \in N_B,\ k \in n_h, \end{aligned} \tag{7}$$

where

$$\widetilde{g}_h(U_{node,hk}) = g_h(U_{node,hk}) Q^r_h, \quad h \in N_B,\ k \in n_h. \tag{8}$$

B. NODAL INJECTIONS

Let $\pi_{i\_\phi,h,k}$ represent the connection of the prosumers to the grid within the given LA:

$$\pi_{i\_\phi,h,k} = \begin{cases} 1/\nu_{h,k} & \text{if the } k\text{-th prosumer of the } h\text{-th category} \\ & \text{is connected in the } i\text{-th grid bus to the} \\ & \phi\text{-th phase, and to } \nu_{h,k} \text{phases in total;} \\ 0 & \text{otherwise.} \end{cases} \tag{9}$$

From (1), (9), the active power injection in the ϕ-th phase of the i–th bus is:

$$P^{inj}_{i\_\phi} = \sum_{h=1}^{n_a+n_b} \sum_{k=1}^{n_h} \pi_{i\_\phi,h,k} P_{h,k} = \sum_{h=1}^{n_a+n_b} P_h \sum_{k=1}^{n_h} \pi_{i\_\phi,h,k}\, p^*_{h,k}$$

$$= \sum_{h=1}^{n_a+n_b} \pi^*_{i\_\phi,h} P_h, \tag{10}$$

with

$$\pi^*_{i\_\phi,h} = \sum_{k=1}^{n_h} \pi_{i\_\phi,h,k} p^*_{h,k}, \quad h \in N_A, N_B,\ k \in n_h. \tag{11}$$

The expression for the reactive injected power is different based on the prosumers' category.

For category N_A, from (3), (9) it is

$$\begin{aligned} Q^{inj}_{i\_\phi} &= \sum_{h=1}^{n_a} \sum_{k=1}^{n_h} \pi_{i\_\phi,h,k} Q_{h,k} \\ &= \sum_{h=1}^{n_a} \widetilde{f}_h(P_h) \sum_{k=1}^{n_h} \pi_{i\_\phi,h,k}\, q^*_{h,k} \\ &= \sum_{h=1}^{n_a} \rho^*_{i\_\phi,h} \widetilde{f}_h(P_h), \quad \phi = 1, 2, 3, \end{aligned} \tag{12}$$

where

$$\rho^*_{i\_\phi,h} = \sum_{k=1}^{n_h} \pi_{i\_\phi,h,k} q^*_{h,k}, \quad h \in N_A. \tag{13}$$

For category N_B, from (7), (9)

$$\begin{aligned} Q^{inj}_{i\_\phi} &= \sum_{h=1}^{n_b} \sum_{k=1}^{n_h} \pi_{i\_\phi,h,k} Q_{h,k} \\ &= \sum_{h=1}^{n_b} \widetilde{g}_h(U_{i\_\phi}) \sum_{k=1}^{n_h} \pi_{i\_\phi,h,k}\, q^*_{h,k} \\ &= \sum_{h=1}^{n_b} \rho^*_{i\_\phi,h}\, \widetilde{g}_h(U_{i\_\phi}), \quad \phi = 1, 2, 3, \end{aligned} \tag{14}$$

where

$$\rho^*_{i\_\phi,h} = \sum_{k=1}^{n_h} \pi_{i\_\phi,h,k} q^*_{h,k}, \quad h \in N_B. \tag{15}$$

From Equations (10), (12) and (14), it is

$$\begin{aligned} \bar{J}^p_{i\_\phi} &= \frac{P^{inj}_{i\_\phi} - j\, Q^{inj}_{i\_\phi}}{\widehat{U}_{i\_\phi}} \\ &= \frac{1}{\widehat{U}_{i\_\phi}} \sum_{h=1}^{n_a} \left(\pi^*_{i\_\phi,h} P_h - j \rho^*_{i\_\phi,h} \widetilde{f}_h(P_h) \right) \\ &\quad + \frac{1}{\widehat{U}_{i\_\phi}} \sum_{h=1}^{n_b} \left(\pi^*_{i\_\phi,h} P_h - j \rho^*_{i\_\phi,h}\, \widetilde{g}_h(U_{i\_\phi}) \right). \end{aligned} \tag{16}$$

For the subsequent development, the value of each voltage is assumed to remain close to that of a reference case for all nodes:

$$\bar{U}_{i\_\phi} \approx \bar{U}^*_{i\_\phi}. \tag{17}$$

Combining (16) and (17) yields

$$\bar{J}^p_{i\_\phi} \approx \frac{1}{\widehat{U}^*_{i\_\phi}} \sum_{h=1}^{n_a} \left(\pi^*_{i\_\phi,h} P_h - j \rho^*_{i\_\phi,h} \widetilde{f}_h(P_h) \right)$$

$$+\frac{1}{\widehat{U}^*_{i\_\phi}}\sum_{h=1}^{n_b}\left(\pi^*_{i\_\phi,h}P_h - j\rho^*_{i\_\phi,h}\widetilde{g}_h(U_{i\_\phi})\right)$$
$$=\sum_{h=1}^{n_a}\dot{\alpha}_{i\_\phi,h}P_h+\dot{\beta}_{i\_\phi,h}\widetilde{f}_h(P_h)$$
$$+\sum_{h=1}^{n_b}\dot{\alpha}_{i\_\phi,h}P_h+\dot{\beta}_{i\_\phi,h}\widetilde{g}_h(U_{i\_\phi}), \tag{18}$$

where

$$\dot{\alpha}_{i\_\phi,h}=\frac{\pi^*_{i\_\phi,h}}{\widehat{U}^*_{i\_\phi}},\quad \dot{\beta}_{i\_\phi,h}=-j\frac{\rho^*_{i\_\phi,h}}{\widehat{U}^*_{i\_\phi}}. \tag{19}$$

III. REDUCED MODELING OF NETWORK

The phase voltages at the LA's edge busses and the currents injected there from the outside into the LA are easily recognized as relevant quantities to represent the LA. In addition, the phase voltages of other, specific busses within the LA may be deemed relevant for monitoring and control purposes; for example, the phase voltages of transformers equipped with OLTC or of DG units operating under voltage control. In the following, relevant nodes/busses are called describing.

Let us focus on the DG plants operating upon volt-var control; the dependence of their reactive injection on the voltage would require to consider the voltages of the busses they are connected to as relevant quantities in the representation of the LA. The number of such plants connected to distribution systems, in particular PV with inverters, is continuously and significantly increasing. It is straightforward to keep all the busses to which such DG plants are connected as 'describing'; however, the size of the network model is quite large and possibly not significantly reduced compared to the whole model. It is therefore desirable to have a model that represents the aforementioned dependence without maintaining all DG busses as describing.

Nodal injected currents are the sum of two contributions: the prosumers'currents (18) and the currents coming from outside the LA, which account for the connection of the LA to the remainder of the system. Only for e nodes there are external injections, while for all other nodes the external injection is zero; recalling that e nodes are included in d nodes and then in D nodes, it can be written:

$$\bar{J}=\bar{J}^{ext}+\bar{J}^{p}=\begin{bmatrix}\begin{bmatrix}\bar{J}_e\\0\end{bmatrix}\\0\end{bmatrix}+\bar{J}^{p}=\begin{bmatrix}\bar{J}_D\\0\end{bmatrix}+\bar{J}^{p}. \tag{20}$$

1) REMOVAL OF THE *in* NODES

From (18) and (20), it is:

$$\bar{J}=\dot{Y}\bar{U}\Rightarrow\begin{bmatrix}\bar{J}_D\\0\end{bmatrix}+\sum_{h=1}^{n_a}\left(\begin{bmatrix}\dot{A}_D\\\dot{A}_{in}\end{bmatrix}_h P_h+\begin{bmatrix}\dot{B}_D\\\dot{B}_{in}\end{bmatrix}_h\widetilde{f}_h(P_h)\right)$$
$$+\sum_{h=1}^{n_b}\left(\begin{bmatrix}\dot{A}_D\\\dot{A}_{in}\end{bmatrix}_h P_h+\begin{bmatrix}\dot{B}_D\odot\widetilde{G}_h(U_D)\\0\end{bmatrix}_h\right)$$
$$\simeq\begin{bmatrix}\dot{Y}_{DD}&\dot{Y}_{D\,in}\\\dot{Y}_{in\,D}&\dot{Y}_{in\,in}\end{bmatrix}\begin{bmatrix}\bar{U}_D\\\bar{U}_{in}\end{bmatrix}. \tag{21}$$

Let (21) be written as

$$\bar{J}_D+\sum_{h=1}^{n_a}\left(\dot{A}_{D,h}P_h+\dot{B}_{D,h}\widetilde{f}_h(P_h)\right)$$
$$+\sum_{h=1}^{n_b}\left(\dot{A}_{D,h}P_h+\dot{B}_{D,h}\odot\widetilde{G}_h(U_D)\right)$$
$$\simeq\begin{bmatrix}\dot{Y}_{DD}&\dot{Y}_{D\,in}\end{bmatrix}\begin{bmatrix}\bar{U}_D\\\bar{U}_{in}\end{bmatrix},$$
$$0+\sum_{h=1}^{n_a}\left(\dot{A}_{in,h}P_h+\dot{B}_{in,h}\widetilde{f}_h(P_h)\right)$$
$$+\sum_{h=1}^{n_b}\left(\dot{A}_{in,h}P_h\right)\simeq\begin{bmatrix}\dot{Y}_{in\,D}&\dot{Y}_{in\,in}\end{bmatrix}\begin{bmatrix}\bar{U}_D\\\bar{U}_{in}\end{bmatrix}. \tag{22}$$

With a Gaussian elimination of $\bar{U}_{in}$ with (22.2), the (22.1) becomes:

$$\bar{J}_D+\sum_{h=1}^{n_a}\left(\dot{\Pi}_{D,h}P_h+\dot{\Psi}_{D,h}\widetilde{f}_h(P_h)\right)$$
$$+\sum_{h=1}^{n_b}\left(\dot{\Pi}_{D,h}P_h+\dot{B}_{D,h}\odot\widetilde{G}_h(U_D)\right)=\dot{\Upsilon}\,\bar{U}_D, \tag{23}$$

where

$$\begin{aligned}\dot{\Pi}_{D,h}&=\dot{A}_{D,h}-\dot{Y}_{D\,in}\,\dot{Y}^{-1}_{in\,in}\,\dot{A}_{in,h},\\ \dot{\Psi}_{D,h}&=\dot{B}_{D,h}-\dot{Y}_{D\,in}\,\dot{Y}^{-1}_{in\,in}\,\dot{B}_{in,h},\\ \dot{\Upsilon}&=\dot{Y}_{DD}-\dot{Y}_{D\,in}\,\dot{Y}^{-1}_{in\,in}\,\dot{Y}_{in\,D}.\end{aligned} \tag{24}$$

A completely reduced representation based on d nodes only as in [13], [14] is not possible here, due to the reactive injection at the q nodes depending on the voltage, in a highly non-linear way. Any representation of the network that gives evidence to d nodes has to take into account this issue for q nodes. In the following, we first derive a model encompassing all D nodes as describing; then, we propose a model with only d nodes as describing, which embeds an approximated linear dependence of reactive generation on the voltage of q nodes and is corrected by means of additional fictitious variables to account for the non-linear dependence.

A. MODEL A—ALL THE D NODES AS DESCRIBING NODES

The terms under summation in (23) introduce errors due to (17); the error can be reduced by considering the actual voltage of the D nodes instead of the reference one [7]:

$$\bar{J}_D+diag\left\{\frac{\widehat{U}^*_{D,i}}{\widehat{U}_{D,i}}\right\}\sum_{h=1}^{n_a}\left(\dot{\Pi}_{D,h}P_h+\dot{\Psi}_{D,h}\widetilde{f}_h(P_h)\right)$$
$$+diag\left\{\frac{\widehat{U}^*_{D,i}}{\widehat{U}_{D,i}}\right\}\sum_{h=1}^{n_b}\left(\dot{\Pi}_{D,h}P_h+\dot{B}_{D,h}\odot\widetilde{G}_h(U_D)\right)$$
$$=\dot{\Upsilon}\,\bar{U}_D; \tag{25}$$

equation (25) is the usual load flow equation for the network reduced to the D nodes, as shown in [13]. Approximations still remain due to (17) for the eliminated *in* nodes, but the

related errors are very low and acceptable from a practical point of view [7].

For the subsequent development, it is useful writing (25) as:

$$\begin{aligned}\bar{J}_d &= \dot{\Upsilon}_{dd}\bar{U}_d + \dot{\Upsilon}_{dq}\bar{U}_q \\ &\quad - diag\left\{\frac{\widehat{U}^*_{d,i}}{\widehat{U}_{d,i}}\right\}\left(\sum_{h=1}^{n_a}\left(\dot{\Pi}_{d,h}P_h + \dot{\Psi}_{d,h}\widetilde{f}_h(P_h)\right)\right. \\ &\quad \left. + \sum_{h=1}^{n_b}\left(\dot{\Pi}_{d,h}P_h + \dot{B}_{d,h}\odot\widetilde{G}_h(U_d)\right)\right), \\ 0 &= \dot{\Upsilon}_{qd}\bar{U}_d + \dot{\Upsilon}_{qq}\bar{U}_q \\ &\quad - diag\left\{\frac{\widehat{U}^*_{q,i}}{\widehat{U}_{q,i}}\right\}\left(\sum_{h=1}^{n_a}\left(\dot{\Pi}_{q,h}P_h + \dot{\Psi}_{q,h}\widetilde{f}_h(P_h)\right)\right. \\ &\quad \left. + \sum_{h=1}^{n_b}\left(\dot{\Pi}_{q,h}P_h + \dot{B}_{q,h}\odot\widetilde{G}_h(U_q)\right)\right). \end{aligned} \tag{26}$$

B. MODEL B–ONLY THE d NODES AS DESCRIBING NODES

Let (23) be written as:

$$\begin{aligned}&\bar{J}_d + \sum_{h=1}^{n_a}\left(\dot{\Pi}_{d,h}P_h + \dot{\Psi}_{d,h}\widetilde{f}_h(P_h)\right) \\ &\quad + \sum_{h=1}^{n_b}\left(\dot{\Pi}_{d,h}P_h + \dot{B}_{d,h}\odot\widetilde{G}_h(U_d)\right) \\ &\quad = \dot{\Upsilon}_{d\,d}\bar{U}_d + \dot{\Upsilon}_{d\,q}\bar{U}_q, \\ &0 + \sum_{h=1}^{n_a}\left(\dot{\Pi}_{q,h}P_h + \dot{\Psi}_{q,h}\widetilde{f}_h(P_h)\right) \\ &\quad + \sum_{h=1}^{n_b}\left(\dot{\Pi}_{q,h}P_h + \dot{B}_{q,h}\odot\widetilde{G}_h(U_q)\right) \\ &\quad = \dot{\Upsilon}_{q\,d}\bar{U}_d + \dot{\Upsilon}_{q\,q}\bar{U}_q. \end{aligned} \tag{27}$$

1) LINEARIZATION FOR q NODES

For the aims of network reduction and solution, it is useful to express $\widetilde{G}_h(\cdot)$ in (27) in a different way for the q nodes.

Let new variables, $\bar{\delta}_{q,h}\, h \in N_B$, be introduced (see Appendix B for details):

$$\bar{\delta}_{q,h} : \widetilde{G}_h(U_q) = \lambda_h\left(\bar{U}_q + \bar{\delta}_{q,h}\right),\ h \in N_B. \tag{28}$$

With (28), the (27.2) can be rewritten as

$$\begin{aligned}&\sum_{h=1}^{n_a}\left(\dot{\Pi}_{q,h}P_h + \dot{\Psi}_{q,h}\widetilde{f}_h(P_h)\right) \\ &\quad + \sum_{h=1}^{n_b}\left(\dot{\Pi}_{q,h}P_h + \lambda_h diag\{\dot{B}_{q,h}\}\left(\bar{U}_q + \bar{\delta}_{q,h}\right)\right) \\ &\quad = \dot{\Upsilon}_{q,de}\bar{U}_d + \dot{\Upsilon}_{q\,q}\bar{U}_q, \end{aligned} \tag{29}$$

which allows obtaining an explicit expression of $\bar{U}_q$:

$$\begin{aligned}\bar{U}_q &= \left(\dot{\Upsilon}_{q\,q} - \sum_{h=1}^{n_b}\lambda_h diag\{\dot{B}_{q,h}\}\right)^{-1} \\ &\quad \times \left(\sum_{h=1}^{n_a}\left(\dot{\Pi}_{q,h}P_h + \dot{\Psi}_{q,h}\widetilde{f}_h(P_h)\right)\right. \\ &\quad \left. + \sum_{h=1}^{n_b}\left(\dot{\Pi}_{q,h}P_h + \lambda_h diag\{\dot{B}_{q,h}\}\bar{\delta}_{q,h}\right) - \dot{\Upsilon}_{q\,d}\bar{U}_d\right). \end{aligned} \tag{30}$$

2) REDUCTION TO d NODES

By substituting (30) in (27.1), we get:

$$\begin{aligned}&\bar{J}_d + \sum_{h=1}^{n_a}\left(\dot{\Pi}^R_{d,h}P_h + \dot{\Psi}^R_{d,h}\widetilde{f}_h(P_h)\right) \\ &\quad + \sum_{h=1}^{n_b}\left(\dot{\Pi}^R_{d,h}P_h + \dot{B}_{d,h}\odot\widetilde{G}_h(U_d) - \dot{L}_h\bar{\delta}_{q,h}\right) \\ &\quad = \dot{\Upsilon}^R_{d\,d}\bar{U}_d, \end{aligned} \tag{31}$$

where

$$\begin{aligned}\dot{X} &= \left(\dot{\Upsilon}_{q\,q} - \sum_{h=1}^{n_b}\lambda_h diag\{\dot{B}_{q,h}\}\right)^{-1}, \\ \dot{\Pi}^R_{d,h} &= \dot{\Pi}_{d,h} - \dot{\Upsilon}_{d\,q}\,\dot{X}\,\dot{\Pi}_{q,h}, \\ \dot{\Psi}^R_{d,h} &= \dot{\Psi}_{d,h} - \dot{\Upsilon}_{d\,q}\,\dot{X}\,\dot{\Psi}_{q,h}, \\ \dot{L}_h &= \lambda_h\dot{\Upsilon}_{d\,q}\,\dot{X}\,diag\{\dot{B}_{q,h}\}, \\ \dot{\Upsilon}^R_{d\,d} &= \dot{\Upsilon}_{d\,d} - \dot{\Upsilon}_{d\,q}\,\dot{X}\,\dot{\Upsilon}_{q\,d}. \end{aligned} \tag{32}$$

Equation (31) is the representation of the whole network with evidence to the d nodes; it is not a completely reduced representation, as the q nodes are still present with their voltages, which must respect (28), (30). The presence of voltage-dependent reactive generation in the q nodes is linearly embedded in the reduced representation (31), and the non-linearities of the volt-var control laws are taken into account through $\bar{\delta}_q$.

The terms under summation in (31) introduce errors due to (17); the error can be reduced by considering the actual voltage of the d nodes instead of the reference one [7]:

$$\begin{aligned}&\bar{J}_d + diag\left\{\frac{\widehat{U}^*_{d,i}}{\widehat{U}_{d,i}}\right\}\left(\sum_{h=1}^{n_a}\left(\dot{\Pi}^R_{d,h}P_h + \dot{\Psi}^R_{d,h}\widetilde{f}_h(P_h)\right)\right. \\ &\quad \left. + \sum_{h=1}^{n_b}\left(\dot{\Pi}^R_{d,h}P_h + \dot{B}_{d,h}\odot\widetilde{G}_h(U_d) - \dot{L}_h\bar{\delta}_{q,h}\right)\right) \\ &\quad = \dot{\Upsilon}^R_{d\,d}\,\bar{U}_d; \end{aligned} \tag{33}$$

equation (33) is a load flow equation for the network reduced to the d nodes [13]. As before, approximations still remain due to (17) for the eliminated nodes, but the related errors are very low and acceptable from a practical point of view.

IV. SOLUTION ALGORITHMS

Various algorithms can be used to solve the models presented in the previous Sect. III, either general purpose or specialized. In all cases, due to the high non-linearity of the volt-var control laws, which have discontinuous derivatives (see Appendix B), the performance of such algorithms can be assessed only with extensive numerical applications.

A. ALGORITHMS FOR MODEL A

For a compact formulation of the algorithms, let functions χ, ψ:

$$\begin{aligned} \chi(\bar{J}_d, \bar{U}_d) &= 0, \\ \psi(\bar{U}_d, \bar{U}_q) &= 0, \end{aligned} \tag{34}$$

formally represent (26.1) and (26.2), respectively.

The non-linear system (34) can be solved as a whole with many existing general purpose methods.

A different, iterative approach can be envisaged; at the k-th iteration, first $\bar{J}_d$, $\bar{U}_d$ are updated by solving (34.1) with $\bar{U}_q$ unchanged, then $\bar{U}_q$ is updated with a scheme based on (34.2):

$$\begin{aligned} \{\bar{J}_d^k,\ \bar{U}_d^k\} : \chi(\bar{J}_d^k,\ \bar{U}_d^k,\ \bar{U}_q^{k-1}) &= 0, \\ \bar{U}_q^k = \bar{U}_q^{k-1} + M^k \psi(\bar{U}_d^k, \bar{U}_q^{k-1}). \end{aligned} \tag{35}$$

The expected computational savings derive from the very small dimension of the non-linear problem encompassed in (35.1), while calculations in (35.2) are straightforward (provided that matrix M^k does not require any inversion); this is counteracted by the iterative nature of the algorithm.

B. ALGORITHM FOR MODEL B

The dimension of the whole representation (28), (30), (33) is bigger than the dimension of model (26); we can expect that solving it as a whole would require even more computational effort, and then we consider an iterative algorithm only.

For a compact formulation of the algorithm, let functions γ, ζ, η:

$$\begin{aligned} \gamma(\bar{J}_d, \bar{U}_d, \bar{\delta}_q) &= 0, \\ \zeta(\bar{U}_d, \bar{U}_q, \bar{\delta}_q) &= 0, \\ \eta(\bar{U}_q, \bar{\delta}_q) &= 0 \end{aligned} \tag{36}$$

formally represent (33), (30), and (28), respectively.

At the k-th iteration of the iterative algorithm, first $\bar{J}_d$, $\bar{U}_d$ are updated by solving (36.1) with $\bar{\delta}_q$ unchanged, then $\bar{U}_q$ is updated through (36.2) still with $\bar{\delta}_q$ unchanged, and finally $\bar{\delta}_q$ is updated with a scheme based on (36.3):

$$\begin{aligned} \{\bar{J}_d^k,\ \bar{U}_d^k\} :\ \gamma(\bar{J}_d^k,\ \bar{U}_d^k,\ \bar{\delta}_q^{k-1}) &= 0, \\ \bar{U}_q^k :\ \zeta(\bar{U}_d^k, \bar{U}_q^k, \bar{\delta}_q^{k-1}) &= 0, \\ \bar{\delta}_q^k = \bar{\delta}_q^{k-1} + N^k \eta(\bar{U}_q^k, \bar{\delta}_q^{k-1}). \end{aligned} \tag{37}$$

Also for this algorithm, the expected computational efficiency is due to the very small dimension of the non-linear problem encompassed in (37.1), while calculations in (37.2) and (37.3) are straightforward (provided that matrix N^k does not require any inversion); once again, this is counteracted by the iterative nature of the algorithm.

V. CASE STUDIES

The case studies analyze the solution of the models A (34) and B (36), for networks of different sizes; the three algorithms discussed in Sect. IV are investigated.

Standard, available algorithms are adopted to find the solution to non-linear equalities (34), or (35.1), or (37.1). For all of them, function *fsolve* available in the Matlab© suite [20] has been adopted. For (34), also an implementation of the quasi-Newton *broyden* algorithm [21] in the Matlab© environment has been tested; no testing with it for (35.1), or (37.1) has been carried out as it would require a specific implementation, which is outside the scope of this work.

The errors introduced by the reduction of the network and the computational effort required to get the solution are illustrated.

The errors in d node voltages among the investigated methods and the original solution are presented for different values of loads and type and location of DG; the errors are considered admissible if they are smaller than the error due to the smallest tap changer step of OLTCs in the grid [11], which corresponds to 0.006250 p.u. for a 32-step voltage regulator with a range of a $\pm 10\%$. The computational effort is presented both in terms of computational time and number of iterations.

The IEEE 123-bus network is considered as the base grid for the analysis; it includes both pure loads and DG. Larger networks are obtained by replicating the base grid (from the same origin) to increase the total number of buses while preserving the structure of the original network. In all cases, network data refer to unbalanced three-phase systems and can be obtained from the IEEE Test feeder [27] and the OpenDSS Simulation Tool [22].

The DG is included in two forms; the first one, DG1, models the reactive power as a function of the active one (see Appendix A); the second one, DG2, contributes to voltage regulation with volt-var control law of category B (see Appendix B). If considered, DG1 covers about 15 % of the total nominal load, with a number of DG generators of about 15 % of the load busses located in the 15 % most loaded three-phase busses. DG2 is considered for two cases: case_1, for a total reactive power equal to 10% of the nominal load reactive power, randomly distributed in 10% of the three-phase busses of the network; case_2, where both the above percentages are 20%.

A. BASE GRID

The network scheme of the base grid 123-bus IEEE test grid is depicted in Fig. 1a. The busses 9r, 25r, and 160 model the tap-changer regulators along the lines [22]; all three-phase transformers are assumed wye-wye, with neutrals grounded. The LAs (Fig. 1b) are identified as in [13], to which the reader

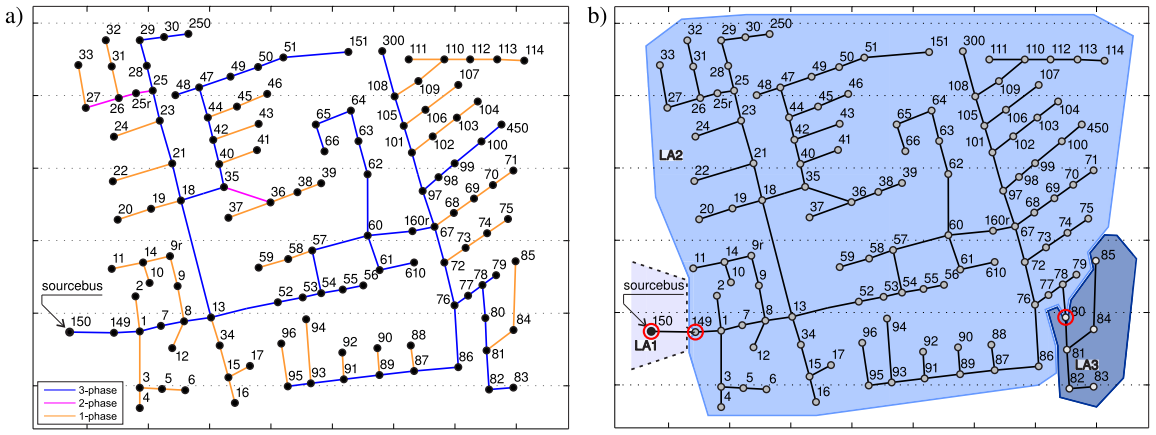

FIGURE 1. Base grid: a) topology – b) LA identification [13].

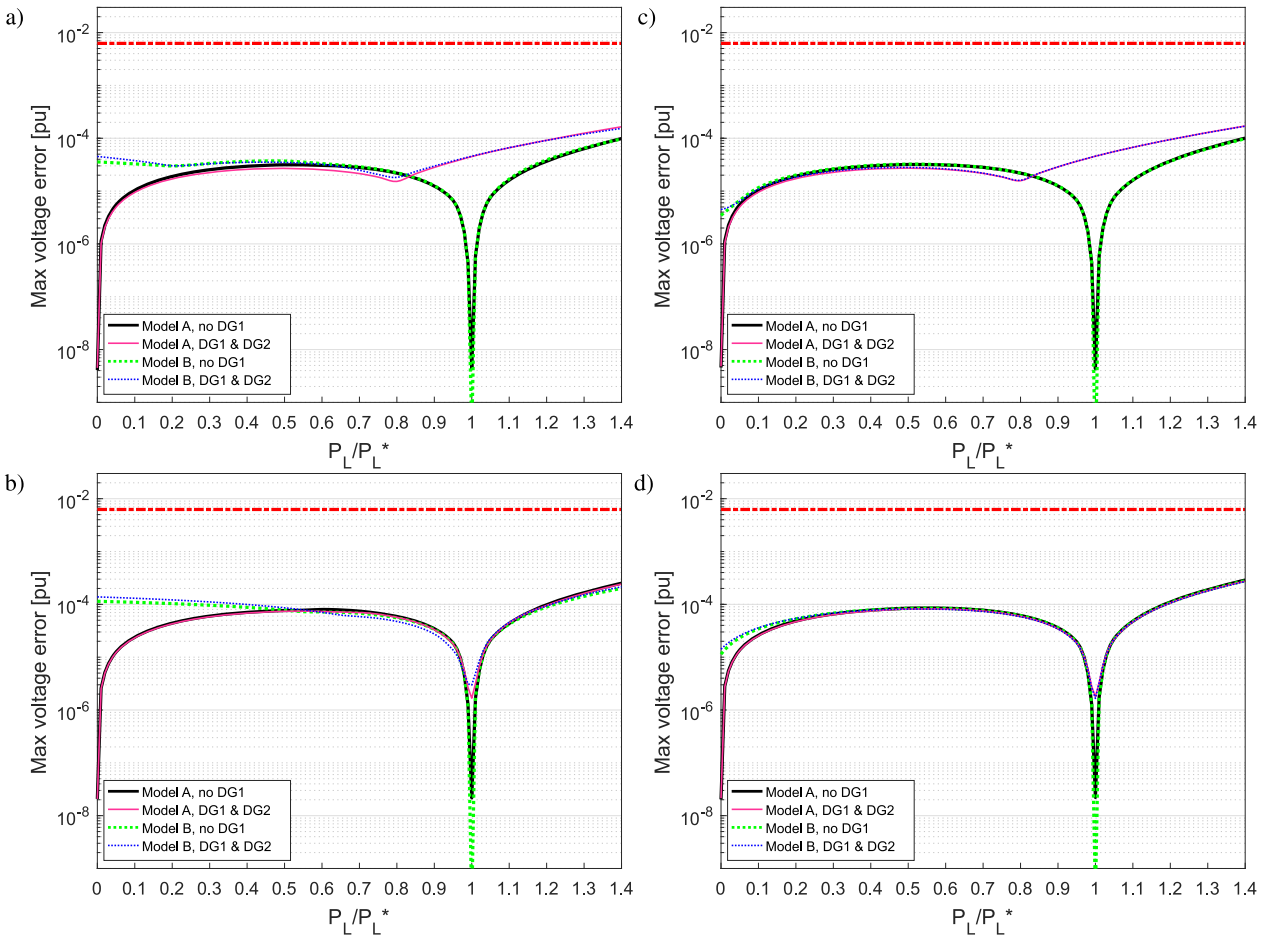

FIGURE 2. Max error in voltages: a) base grid, case_1 – b) base grid, case_2 – c) x10 – case_1 – d) x10, case_2.

is referred for more details. The reduced representations of each ot the three resulting LAs is obtained as in Sect. III; the composition of the three reduced LA models leads to a reduced representation of the entire grid made of three busses (150, 149, 80 – red circles in Fig. 1b).

For the solution of model A (34) with algorithm (35), matrix M^k has been taken diagonal and constant; after some numerical experiments, irrespective of presence of DG1 good values have been found $M^k = 1.560\,I$ for case_1 and $M^k = 1.375\,I$ for case_2. For the solution of model B (36) with algorithm (37), also matrix N^k has been taken diagonal and constant; irrespective of presence of DG1, good values have been found $N^k = (0.83/\lambda_h)I$ and $N^k = (0.85/\lambda_h)I$ for case_1 and case_2, respectively.

TABLE 1. Mean time and number of iterations to solve the reduced modeling of the network ($a_c = 10^{-6}$).

case_1

	model	algorithm	method	grid size			
				base	×3	×5	×10
time to solve [s]	A	(34)	*fsolve*	0.30	2.29	5.58	20.98
			broyden	0.07	0.54	1.32	4.85
		(35)	*d fsolve*, *q* iterative	0.36	0.63	0.80	1.25
	B	(37)	*d fsolve*, δ iterative	0.09	0.21	0.31	0.79
iterations	A	(34)	*fsolve*	1	1	1	1
			broyden	1	1	1	1
		(35)	*d fsolve*, *q* iterative	23	23	23	23
	B	(37)	*d fsolve*, δ iterative	9	9	9	9

case_2

	model	algorithm	method	grid size			
				base	×3	×5	×10
time to solve [s]	A	(34)	*fsolve*	0.77	6.72	17.26	49.01
			broyden	0.21	1.62	4.21	14.99
		(35)	*d fsolve*, *q* iterative	1.48	2.28	3.09	4.60
	B	(37)	*d fsolve*, δ iterative	0.10	0.24	0.44	1.11
iterations	A	(34)	*fsolve*	1	1	1	1
			broyden	1	1	1	1
		(35)	*d fsolve*, *q* iterative	77	77	77	77
	B	(37)	*d fsolve*, δ iterative	14	15	15	15

Figures 2a-2b report in log scale the maximum voltage errors of the reduced models versus the total load, with and without DG1, respectively for case_1 and case_2; in all cases the errors result far below the admissibility threshold (red dot-line). The high penetration of DG2 of case_2 does not significantly affect the voltage error; consider that in case_2 there is a high number of *q* nodes, whose voltage is explicitly computed. It can be noticed that the errors with model A and model B are different depending on the passive load and the penetration of DG; in all cases, the errors stay well below the admissibility threshold.

Table 1 reports computational time and number of iterations required to solve the different models with the different algorithms.

For model *A*, the problem is solved faster by handling the *d*-*q* problem in its entirety (34), and *broyden* performs best. For model *B*, the computational time is slightly higher than *broyden* in case_1, while it is about half in case_2. The computational time per iteration in the iterative approaches (35) and (37) is much lower than that of the single iteration required for solving the problem as a whole (34), while the number of iterations is higher.

The comparison of the number of iterations between (35) and (37) is always in favor of the latter.

Model *B* (36) with algorithm (37) behaves very well; it is apparent that in the base grid the solution time is close to the best for model A (34) for case_1, and it is better when the complexity of the problem grows as in case_2, with an increased number of volt-var control busses.

B. LARGE-SIZE NETWORKS

Numerical tests for large networks are carried out by replicating the base grid 3, 5, and 10 times, from the same origin. The identification and reduced representation of LAs is carried out as for the base grid.

For matrices M^k and N^k the same values as the base grid are used. No significant difference in the voltage errors emerged among the medium and large grids (see Figs. 2c-2d).

In contrast, the time required to get the solution is strongly affected by the network size, especially for model *A* solved as a whole. For model *A* the iterative algorithm (35) performs better than solving the problem as a whole (34), starting from size x3, for *fsolve*, and from size x5, for *broyden*; this is due to

the smaller computational time per iteration, which becomes relevant for these network sizes.

Concerning model B, it is always the best in terms of computational times, showing growing advantages as the size and the complexity of the network grow.

C. SOME CONSIDERATIONS

Case studies evidence that model A (34) and model B (36) show similar accuracy results, but their solution requires different computational efforts. The solution of model A treated as a whole is preferable for small to moderate size grids. In contrast, the iterative algorithms show better performance for big grids, where the low computational time per iteration becomes the dominant factor.

It is also apparent that model B (iteratively solved) has to be preferred, as it generally ensures the best results in terms of computational time, putting together the low number of non-linear equalities to be solved with a low number of iterations. The latter can be explained with the (approximated) linear embedding of voltage-dependent reactive generation for the q nodes in the representation of the network reduced to d nodes.

VI. CONCLUSION

The paper proposes two methods to obtain and solve a reduced model of a distribution system in the presence of numerous devices with voltage-controlled power injection, which limits the degree of network reduction possible with traditional methods.

Focusing on volt-var control, the first method is based on the usual modeling of the control laws and on solving the reduced network model with a specialized iterative algorithm; in the second method, a new representation of control laws is proposed together with a specialized iterative algorithm.

Numerical results are presented for four unbalanced test cases of different sizes, highlighting the acceptability of the approximations introduced by the proposed reduced models and the computational aspects associated with the solution of the reduced network model. The results, presented both with graphs and tables, give clear evidence of the beneficial characteristics of the second method, which is the preferred choice.

APPENDIX A
Q-P RELATIONSHIPS

We report here the $Q - P$ relationships already presented in [8], [13], to which the reader is referred for more details.

The active power injection by the k-th prosumer in the h-th category is given by (1), reported here for an easy reference:

$$P_{h,k} = p^*_{h,k} P_h, \quad \forall h, \ \forall k. \tag{38}$$

The general expression for the reactive power injection is (2), also reported here for an easy reference:

$$Q_{h,k} = q^*_{h,k} f_h(P_h) P_h, \quad \forall h, \ \forall k. \tag{39}$$

A. PURE LOADS

A constant power factor (pf) can be assumed, which allows to write:

$$Q_{h,k} = \tan \varphi^*_{h,k} P_{h,k}, \quad h \equiv \text{pure loads}, \tag{40}$$

with apparent meaning of $\tan \varphi^*_{h,k}$. From Equations (38) and (40) it is:

$$Q_{h,k} = \tan \varphi^*_{h,k} \, p^*_{h,k} \, P_h, \quad h \equiv \text{pure loads}, \tag{41}$$

which can be written as (39) with

$$q^*_{h,k} = \tan \varphi^*_{h,k} \, p^*_{h,k}, \quad f_h(P_h) = 1, \quad h \equiv \text{pure loads}. \tag{42}$$

B. DISTRIBUTED GENERATION

Also for DG, the active power injection by the k-th plant in the h-th DG category can expressed with (38): in a given region, the DG plants of a given category (for example, PV or wind) generate active power in a similar way. For reactive power, the size of the DG plant has to be taken into account, as in the following.

Small-size DG plants normally operate at unitary pf [23]. The reactive power injection by the k-th DG plant in the small-size-DG category is obtained simply as follows:

$$Q_{h,k} = 0, \quad h \equiv \text{small DG}, \tag{43}$$

which can be written as (39) with

$$q^*_{h,k} = n.a., \quad f_h(P_h) = 0, \quad h \equiv \text{small DG}. \tag{44}$$

Medium-to-large-size DG plants are connected to MV or HV distribution systems. It is often required that their reactive power injection is made dependent on the active one, so that the plants participate in keeping an acceptable voltage profile. For example, DG plants equipped with static converters should have the pf depicted in Fig. 3 [18].

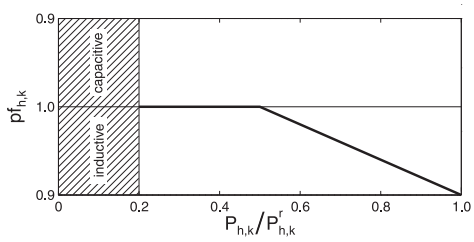

FIGURE 3. Power factor characteristic for medium/large DG plants [8].

Since

$$\frac{P_{h,k}}{P^r_{h,k}} = \frac{p^*_{h,k} P_h}{p^*_{h,k} P^r_h} = \frac{P_h}{P^r_h}, \tag{45}$$

the pf-to-P dependency is the same for all the plants in the same medium-to-large DG category:

$$\text{pf}_{h,k}(P_{h,k}) = \text{pf}_h(P_h). \tag{46}$$

From (38) and (46), the reactive power injection by the k-th plant in the medium-to-large size DG category can be expressed as follows:

$$Q_{h,k} = \tan\left(\arccos(\mathrm{pf}_h(P_h))\right) p^*_{h,k}\, P_h, \quad h \equiv \text{medium to large DG}; \tag{47}$$

equation (47) can be written as (39) with

$$q^*_{h,k} = p^*_{h,k}, \quad f_h(P_h) = \tan\left(\arccos(\mathrm{pf}_h(P_h)\right), \quad h \equiv \text{medium to large DG}. \tag{48}$$

APPENDIX B
VOLT-VAR CONTROL LAWS

Distributed generators may be required to participate in the voltage regulation. This is accomplished by DG inverters which autonomously modify their reactive power based on the local voltage.

Volt-var control laws are various, based on either the ability/necessity by the DG to participate into the voltage regulation [19] or the rated power of DG [18]. Figure 4 shows examples of the control laws proposed in [19] for the two DG categories of minimum performance (Category A) and extended requirements (Category B); they have been drawn so as to give evidence to function $g_h(\cdot)$ (see (4), (5)):

$$g_h(U_{node,hk}) = \frac{Q_h}{Q^r_h} = \frac{Q_{h,k}}{Q^r_{h,k}} = g_{h,k}(U_{node,hk}), \quad h \in N_B,\ k \in n_h. \tag{49}$$

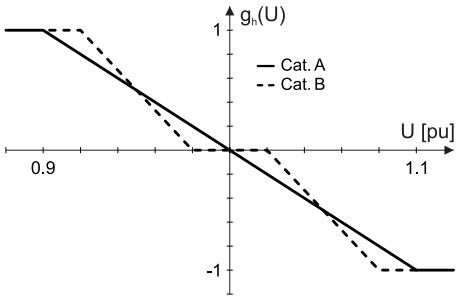

FIGURE 4. Volt-var control proposed in [19].

Fig. 5 shows examples of the control laws proposed in [18] for the rated power of the power park module up to 6 MW or more than 6 MW. Also in Fig. 5 evidence is given to function $g_h(\cdot)$ in (49).

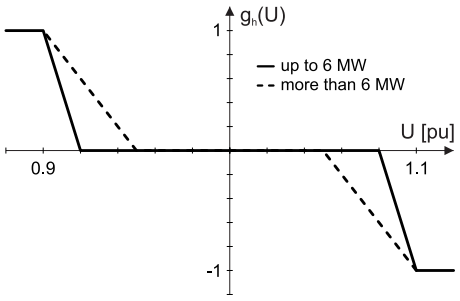

FIGURE 5. Volt-var control proposed in [18].

A. LINEARIZATION

Control laws $g_h(\cdot)$ are apparently non-linear; they can be expressed as the sum of a linear component and a nonlinear one by introducing some fictious voltages.

New variables $\delta_h\ \forall h$ can be defined such that

$$\delta_h : g_h(U) = s_g\,(U + \delta_h)\ \ \forall h; \tag{50}$$

from Figs. 4 and 5 it is apparent that in normal operating condition, $0.9 \le U \le 1.1$, all control laws $g_h(\cdot)$ have the same mean slope, s_g, and $s_g = -10\,\frac{pu}{pu}$.

In the development of the reduced model in Section III-B1, it is useful to express the voltage-controlled reactive generation (for q nodes) versus voltage phasor instead of voltage amplitude. It can be easily accomplished with:

$$\bar{\delta}_h : g_h(U) = s_g\left(\bar{U} + \bar{\delta}_h\right)\ \ \forall h, \tag{51}$$

which is (28) with:

$$\lambda_h = s_g\, Q^r_h \quad \forall h. \tag{52}$$

REFERENCES

[1] Z. K. Pecenak, V. R. Disfani, M. J. Reno, and J. Kleissl, "Multiphase distribution feeder reduction," *IEEE Trans. Power Syst.*, vol. 33, no. 2, pp. 1320–1328, Mar. 2018.

[2] A. Nagarajan, A. Nelson, K. Prabakar, A. Hoke, M. Asano, R. Ueda, and S. Nepal, "Network reduction algorithm for developing distribution feeders for real-time simulators," in *Proc. IEEE Power Energy Soc. Gen. Meeting*, Jul. 2017, pp. 1–5.

[3] X. Lu, W. Wang, and J. Ma, "An empirical study of communication infrastructures towards the smart grid: Design, implementation, and evaluation," *IEEE Trans. Smart Grid*, vol. 4, no. 1, pp. 170–183, Mar. 2013.

[4] Y. Yan, Y. Qian, H. Sharif, and D. Tipper, "A survey on smart grid communication infrastructures: Motivations, requirements and challenges," *IEEE Commun. Surveys Tuts.*, vol. 15, no. 1, pp. 5–20, Feb. 2013.

[5] R. Belhomme, R. C. R. De Asua, G. Valtorta, A. Paice, F. Bouffard, R. Rooth, and A. Losi, "ADDRESS–active demand for the smart grids of the future," in *Proc. CIRED Seminar, SmartGrids Distrib.*, Jun. 2008, pp. 1–4.

[6] G. M. Casolino, A. R. Di Fazio, A. Losi, and M. Russo, "Smart modeling and tools for distribution system management and operation," in *Proc. IEEE Int. Energy Conf. Exhib. (ENERGYCON)*, Sep. 2012, pp. 635–640.

[7] G. M. Casolino and A. Losi, "Load area model accuracy in distribution systems," *Electr. Power Syst. Res.*, vol. 143, pp. 321–328, Feb. 2017.

[8] G. M. Casolino and A. Losi, "Load areas in distribution systems," in *Proc. IEEE 15th Int. Conf. Environ. Electr. Eng. (EEEIC)*, Jun. 2015, pp. 1637–1642.

[9] J. B. Ward, "Equivalent circuits for power-flow studies," *Trans. Amer. Inst. Electr. Eng.*, vol. 68, no. 1, pp. 373–382, Jul. 1949.

[10] H. Oh, "A new network reduction methodology for power system planning studies," *IEEE Trans. Power Syst.*, vol. 25, no. 2, pp. 677–684, May 2010.

[11] A. B. Eltantawy and M. M. A. Salama, "A novel zooming algorithm for distribution load flow analysis for smart grid," *IEEE Trans. Smart Grid*, vol. 5, no. 4, pp. 1704–1711, Jul. 2014.

[12] A. P. Reiman, T. E. McDermott, M. Akcakaya, and G. F. Reed, "Electric power distribution system model simplification using segment substitution," *IEEE Trans. Power Syst.*, vol. 33, no. 3, pp. 2874–2881, May 2018.

[13] G. M. Casolino and A. Losi, "Load areas in radial unbalanced distribution systems," *Energies*, vol. 12, no. 15, p. 3030, Aug. 2019. Accessed: Sep. 16, 2020. [Online]. Available: https://www.mdpi.com/1996-1073/12/15/3030

[14] G. M. Casolino and A. Losi, "Reduced modeling of unbalanced radial distribution grids in load area framework," *IEEE Access*, vol. 8, pp. 179931–179941, 2020.

[15] Z. K. Pecenak, H. V. Haghi, C. Li, M. J. Reno, V. R. Disfani, and J. Kleissl, "Aggregation of voltage-controlled devices during distribution network reduction," *IEEE Trans. Smart Grid*, vol. 12, no. 1, pp. 33–42, Jan. 2021.
[16] H. Kikusato, T. S. Ustun, J. Hashimoto, and K. Otani, "Aggregate modeling of distribution system with multiple smart inverters," in *Proc. Int. Conf. Smart Energy Syst. Technol. (SEST)*, Sep. 2019, pp. 1–6.
[17] P. Koponen, J. Ikäheimo, A. Vicino, A. Agnetis, G. D. Pascale, N. R. Carames, J. Jimeno, E. F. Sánchez-Úbeda, P. Garcia-Gonzalez, and R. Cossent, "Toolbox for aggregator of flexible demand," in *Proc. IEEE Int. Energy Conf. Exhib. (ENERGYCON)*, Sep. 2012, pp. 623–628.
[18] *Reference Technical Rules for the Connection of Active and Passive Consumers to the HV and MV Electrical Networks of Distribution Company*, (in Italian), Norma Italiana CEI, Comitato Elettrotecnico Italiano, Milan, Italy, 2019.
[19] *IEEE Standard for Interconnection and Interoperability of Distributed Energy Resources With Associated Electric Power Systems Interfaces*, IEEE Standard 1547-2018, 2018, pp. 1–138.
[20] *MATLAB Optimization Toolbox*, MATLAB, MathWorks, Natick, MA, USA, 2018.
[21] A. Mjaavatten. *Nonlinear Equation System Solver: Broyden, MATLAB Central File Exchange*. Accessed: Jun. 15, 2021. [Online]. Available: https://www.mathworks.com/matlabcentral/fileexchange/54667-nonlinear-equation-system-solver-broyden
[22] EPRI. *OpenDSS Simulation Tool*. Accessed: Sep. 16, 2020. [Online]. Available: http://smartgrid.epri.com/SimulationTool.aspx
[23] *Reference Technical Rules for the Connection of Active and Passive Users to the LV Electrical Utilities*, (in Italian), Norma Italiana CEI, Comitato Elettrotecnico Italiano, Milan, Italy, 2019.

GIOVANNI MERCURIO CASOLINO (Member, IEEE) received the Graduate degree (Hons.) in electrical engineering and the Ph.D. degree in electrical engineering and information technology from the University of Cassino and Southern Lazio, Cassino, Italy, in 1999 and 2004, respectively. He is currently an Assistant Professor with the University of Cassino and Southern Lazio, where he teaches courses in the power systems area. He is the coauthor of international scientific publications on the modeling of distribution systems by load areas, on the optimal management of the deregulated electricity market, on object-oriented methods for state estimation in distribution networks, on unit commitment, and voltage regulation in presence of distributed generation.

ARTURO LOSI was born in Naples, Italy. He received the master's and Ph.D. degrees in electrical engineering from the University of Naples. Since 1988, he has been working with the Faculty of Engineering, University of Cassino and Southern Lazio, where he has been a Full Professor, since 2000. He has carried out research and teaching activities in the USA and Hong Kong. His research interests include modeling and optimization of power systems, and teach courses in the same area. He was the Department Chair, a member of the governing bodies of an international research consortium, and the Chair of an Italian inter-university consortium.